

Evolving Fuzzy System Applied to Battery Charge Capacity Prediction for Fault Prognostics

***Murilo Camargos^a** and **Iury Bessa^{a,b}** and **Luiz A. Q. Cordovil Junior^a** and **Pedro Coutinho^a**
and **Daniel Furtado Leite^c** and **Reinaldo Martinez Palhares^d**

^aGraduate Program in Electrical Engineering, Federal University of Minas Gerais, Brazil,
{murilo.camargosf, luiz.cordovil05, coutinho.p92}@gmail.com

^bDepartment of Electricity, Federal University of Amazonas, Brazil, iurybessa@ufam.edu.br

^cDepartment of Automatics, Federal University of Lavras, Brazil, daniel.leite@ufla.br

^dDepartment of Electronics Engineering, Federal University of Minas Gerais, Brazil,
rpalhares@ufmg.br

Abstract

This paper addresses the use of data-driven evolving techniques applied to fault prognostics in Li-ion batteries. In such problems, accurate predictions of multiple steps ahead are essential for the Remaining Useful Life (RUL) estimation of a given asset. The fault prognostics' solutions must be able to model the typical nonlinear behavior of the degradation processes of these assets, and be adaptable to each unit's particularities. In this context, the Evolving Fuzzy Systems (EFSs) are models capable of representing such behaviors, in addition of being able to deal with non-stationary behavior, also present in these problems. Moreover, a methodology to recursively track the model's estimation error is presented as a way to quantify uncertainties that are propagated in the long-term predictions. The well-established NASA's Li-ion batteries data set is used to evaluate the models. The experiments indicate that generic EFSs can take advantage of both historical and stream data to estimate the RUL and its uncertainty.

Keywords: Data-driven RUL estimation, Fault prognostics, Evolving fuzzy systems, Takagi–Sugeno fuzzy models.

Acronyms

exTS	Evolving Extended Takagi-Sugeno
RUL	Remaining Useful Life
PHM	Prognostics and Health Management
EBeTS	Error Based Evolving Takagi-Sugeno Model
CBM	Condition-based Maintenance

HI	Health Index
TS	Takagi-Sugeno
UUT	Unit Under Test
MF	Membership Function
RLS	Recursive Least Squares
MAPE	Mean Absolute Percentage Error
RA	Relative Accuracy
FT	Fault Threshold
ARMA	Autoregressive Moving Average
eMG	Evolving Multivariable Gaussian
EFS	Evolving Fuzzy System

1 Introduction

Li-ion batteries empowers many applications that are present in our lives; from small devices such as our cell phones to bigger machines such as electric vehicles. This wide range of applications drives increasing investments to create new maintenance policies that can prevent unexpected failures. These policies are in continuous improvement towards reliability and cost-effectiveness. Between preventive and corrective maintenance strategies, Condition-based Maintenance (CBM) is developed to be the optimal point in terms of total costs, balancing operating with maintenance costs.

A key CBM program is the Prognostics and Health Management (PHM), which creates relevant health indicators out of monitoring data to reduce inspections through early fault detection and prediction of impending faults [12]. Health prognostics is a primary task in this context and consists of predicting the Remaining Useful Life (RUL) of these machines [15]. The RUL prediction methodologies are commonly classified into three categories: data-driven, model-based, and hybrid. The latter combines characteristics of the former two categories [13]. Model-based approaches

rely on first-principle models to assess the RUL [8]. Although these models tend to outperform models in other categories, they may be challenging to obtain in practical situations, and reusing these models in different assets may be impossible [15].

The drawbacks of first-principle methods motivate the development of data-driven approaches based on statistical models and artificial intelligence techniques. Particularly, artificial intelligence approaches deal with complex systems by learning how to produce the desired outputs from given inputs, i.e., learning input-output relationships, which are possibly nonlinear [1]. However, it is usually necessary to retrain artificial intelligence models if the operating conditions change [23]; and the algorithms usually require a large amount of high-quality training data.

In general, data-driven approaches have fixed structures, i.e., they assume stationary environment. Such assumption often does not hold, making the aforementioned approaches unsuitable for real-time prognostics, where human intervention is not always possible to redefine the problem domain if needed. A way of tackling the stationarity assumption is to develop strategies based on multiple models [7]. The multiple model strategy can be automated by developing evolving models, whose knowledge-base is built based on data streams, allowing the learning of complex behaviors and novelties from scratch [6]. The ability to model complex nonlinear dynamics in non-stationary environments places the Evolving Fuzzy Systems (EFSs) as interesting choices for prognostics applications in cases where it is rough to represent or describe time-varying and nonlinear characteristics of a system. Nonetheless, literature on applying evolving intelligence to fault prognostic issues is somewhat scarce; a subset of that addresses the uncertainty quantification problem [3, 9, 10, 24].

The practical applications of EFSs are various. Their recursive nature allows real-time fault detection and diagnosis [17, 19], systems identification, and time-series prediction [16]. The present study focuses on system identification and time-series prediction problems in which the majority of the existing models are based on variations of Takagi-Sugeno (TS) fuzzy inference systems, i.e., models whose rules consist of functional consequent terms. In their evolving formulations, these models display a fully adaptive structure in terms of the number of rules, and antecedent and consequent parameters through data-streams. Online learning is supported by a recursive incremental learning mechanism that decides about rule creation, exclusion, updating, and merging.

Throughout the years, different kinds of EFSs have

been proposed to explore nuances of different learning mechanisms. The multivariable model called Evolving Extended Takagi-Sugeno (exTS) [2] partitions the input/output data space through an extension of the concepts of subtractive clustering [5]. The learning process of creating and excluding rules in the knowledge-base is related to recursively computed quality metrics such as the zone of influence of each cluster, their age, and support size. Local models are constructed by means of univariate Gaussian Membership Functions (MFs) for each premise variable.

The application of evolving models for time series prediction and systems identification has stimulated efforts towards the development of models that account for complex relationships among input variables. The EFS called Evolving Multivariable Gaussian (eMG) uses first-order functions and multivariate Gaussians as MF to represent the premise variables [18]. This kind of MF can model the relation among input variables through the recursive computation of a dispersion matrix. The model uses a learning mechanism based on the participatory learning principle that endows the algorithm with the capacity to classify whether a sample is an outlier or the first representative of a new cluster [30].

Due to a clear relation between the prognostics task addressed in this paper and long-term forecasting, the Error Based Evolving Takagi-Sugeno Model (EBeTS) is considered. EBeTS combines multivariate Gaussians – to represent complex relationships among input variables – with criteria designed to explicitly take advantage of the estimation error to update the model's structure on the fly [3]. The choice of hyper-parameters in EBeTS can be made in a fully problem-agnostic way, which facilitates its application in different problems, such as the prognostics of rolling bearings and Li-ion batteries. Reference [3] also provides a framework that enables the use of different EFSs in prognostics tasks in which model's uncertainty must be considered. The main contributions of the present paper are the following:

1. Fault prognostics is performed taking into consideration the Li-ion battery dataset and EFSs;
2. The uncertainty quantification procedure proposed in [3] is improved by means of a more stable quantification of the model's initial error;
3. The RUL's confidence bounds were generalized as z-values of the normal distribution computed through a given significance level.

The remainder of this paper is organized as follows. Section 2 states the prognostics problem by provid-

ing the definition of RUL used in this paper. Section 3 describes the computational framework that supports EFSs for long-term prediction as well as the novel uncertainty quantification procedure, which allows the computation of confidence intervals using fuzzy TS models. In Section 4, a real benchmark dataset, namely, the Li-ion battery charging dataset, provided by NASA, and a parameter tuning procedure to test prognostics approaches are presented. Section 5 shows the results and discusses the application of three different EFSs and a non-evolving model for fault prognostics. Finally, Section 6 concludes the paper.

2 The prognostics problem

RUL prediction is an essential step in prognostics. Based on the asset's age and condition, and on previous operation profile, RUL prediction concerns estimating how much time remains, from the current instant, to a possible fault occurrence [11]. Some authors define RUL from the Health Index (HI) point of view, i.e., RUL is the time left until the system's degradation state reaches a given Fault Threshold (FT) [20, 28], which is expressed by:

$$\hat{r}_k = \inf \{N \in \mathbb{N} | \hat{x}_{k+N} \geq \eta\}, \quad (1)$$

where \hat{r}_k denotes the RUL computed at instant k , given observations of the degradation state until k ; \mathbb{N} is the natural numbers set; \hat{x}_{k+N} is an estimate of the degradation state, i.e., the HI at time $k + N$; and η is the predefined FT.

In addition to a pointwise RUL estimate, providing a confidence interval in which the RUL belongs – which takes into consideration the inherent uncertainty of fault prognostics [29] – is equally important. An example of uncertainty in RUL estimate is shown in Figure 1. Notice that the predicted degradation path reaches the FT (blue dot) before the actual degradation path does (red dot). However, a confidence interval extracted from a probability density function around the pointwise estimate encloses the true RUL. Another uncertain value in RUL prediction is related to the FT itself. The FT can also be described by means of a probability distribution – or *failure domain*. However, in a great part of the literature, including the present paper, the FT is represented by a constant line to simplify the RUL prediction process [15]. Therefore, Eq. (1) is a simplified version of the canonical RUL definition by [4], where the concept of failure domain is defined.

The state of a system deteriorates until it reaches the FT, namely η . Thus, we define the RUL prediction problem in this paper as a multi-step-ahead prediction

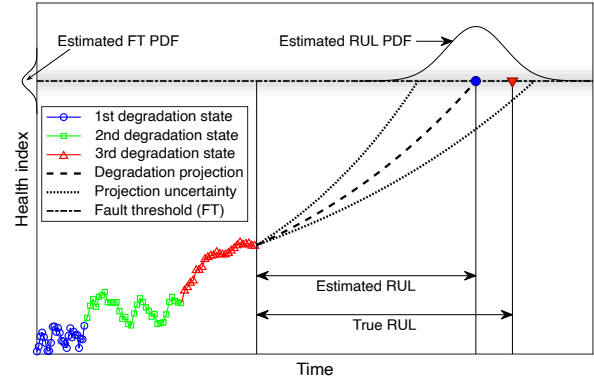


Figure 1: Degradation stages and uncertainty in RUL prediction.

problem; we want to estimate η . State propagation can be performed using the following state transition relation,

$$\hat{x}_{k+N|k} = f_k(\mathbf{v}_{k+N,L}, \boldsymbol{\varepsilon}_{k+N}), \quad (2)$$

in which $\mathbf{v}_{k+N,L}$, given by

$$\mathbf{v}_{k+N,L}^\top = \begin{cases} [x_k & x_{k-1} & \cdots & x_{k-L+1}], & \text{if } N = 1 \\ [\hat{x}_{k+N-1} & \cdots & \hat{x}_{k+1} & x_k & \cdots & x_{k+N-L}], & \text{if } 2 \leq N \leq L \\ [\hat{x}_{k+N-1} & \cdots & \hat{x}_{k+N-L}], & \text{if } N > L \end{cases} \quad (3)$$

is a lag vector with estimates; $\boldsymbol{\varepsilon}_k$ is an independent identically distributed (i.i.d.) noise vector. Furthermore, x_n and \hat{x}_n are, respectively, the observed and estimated degradation state at the time step n ; L is the order of the auto-regression polynomial; N is the number of steps ahead for which the degradation state is predicted; and $f_k(\cdot)$ is the state transition function recursively obtained up to the instant k using an EFS. In this paper, long-term estimates are given by the iterative approach [10] due to its simple implementation and quickness. Moreover, establishing a prediction horizon is needless. The iterative approach performs one-step prediction, and uses the last predicted value as a regressor to estimate the next value.

3 Data-driven prognostics with EFS

A TS fuzzy model allows the representation of a system by means of fuzzy concepts. The TS fuzzy model uses functional consequent, usually linear [22]. In such systems, given a set of C rules, the i -th **IF-THEN** rule, is

$$\text{Rule } i: \text{ IF } \mathbf{x}_k \text{ IS } \Phi_{i,k-1} \text{ THEN } \hat{y}_{i,k} = \tilde{\mathbf{x}}_k^\top * \hat{\boldsymbol{\theta}}_{i,k-1} \quad (4)$$

where $\mathbf{x}_k \in \mathbb{R}^{n_x}$ is the vector of premise variables, $\hat{\boldsymbol{\theta}}_{i,k-1} \in \mathbb{R}^{n_x+1}$ is the vector of estimated consequent parameters, and $\tilde{\mathbf{x}}_k = [1 \quad \mathbf{x}_k^\top]^\top$. Moreover, $\mathbf{x}_k \text{ IS } \Phi_{i,k-1}$ denotes the fuzzy relation between \mathbf{x}_k and

the fuzzy set $\Phi_{i,k-1}$ for $i \in \mathbb{N}_{\leq C}$, such that the multivariate MF is $\varphi_{i,k-1}: \mathbb{R}^{n_x} \rightarrow [0, 1]$. Throughout the text, $\mathbb{N}_{\leq k}$ will be used to denote the set of natural numbers up to k , such that $\mathbb{N}_{\leq k} = \{1, 2, \dots, k\}$.

The output of the TS fuzzy model is a convex combination among C consequent linear models weighted by the rules' activation degrees. Activation degrees must comply with the convex sum property, i.e., they need to be non-negative and sum one. From the center average defuzzification, the overall model output is given as

$$\hat{y}_k = \sum_{i=1}^C h_{i,k-1}(\mathbf{x}_k) \hat{y}_{i,k} \quad (5)$$

in which

$$h_{i,k-1}(\mathbf{x}_k) = \frac{\varphi_{i,k-1}(\mathbf{x}_k)}{\sum_{m=1}^C \varphi_{m,k-1}(\mathbf{x}_k)}. \quad (6)$$

When using univariate MFs, rules' activation degrees are obtained from aggregation operator based on a t-norm. At instant k , the system output (5) can be rewritten in matrix form as

$$\hat{y}_k = \mathbf{h}_{k-1}^\top(\mathbf{x}_k) \hat{\Theta}_{k-1}^\top \tilde{\mathbf{x}}_k, \quad (7)$$

where $\mathbf{h}_{k-1}(\mathbf{x}_k) = [h_{1,k-1}(\mathbf{x}_k) \ \dots \ h_{C,k-1}(\mathbf{x}_k)]^\top \in \mathbb{R}^C$ is the vector of normalized activation degrees, and $\hat{\Theta}_{k-1} = [\hat{\theta}_{1,k-1} \ \dots \ \hat{\theta}_{C,k-1}]^\top \in \mathbb{R}^{n_x+1 \times C}$ is the matrix of consequent coefficients, as estimated in the previous time step using Recursive Least Squares (RLS).

Given a number of rules, C , the TS model creates a coarse fuzzy partitioning of the data space, and updates the parameters of first-order consequent functions to locally approximate the behavior of a system. An issue on online stream modeling concerns the lack of *a priori* knowledge about the model structure, i.e., its number of rules [14]. This is particularly relevant in fault prognostics since degradation dynamics are typically nonlinear, non-stationary, and different for each Unit Under Test (UUT).

3.1 Uncertainty estimation

Consider a state transition function given by a TS model, with rules as in (4). The degradation propagation (2) can be rewritten as

$$\hat{\mathbf{x}}_{k+N} = \mathbf{h}_k^\top(\mathbf{v}_{k+N,L}) \hat{\Theta}_k^\top \tilde{\mathbf{v}}_{k+N,L} + \boldsymbol{\varepsilon}_{k+N}, \quad \forall N > 0 \quad (8)$$

where $\mathbf{h}_k(\cdot)$ and $\hat{\Theta}_k$ are the normalized degrees of activation and consequent parameters for each rule with structure updated until time instant k ; N is the prediction horizon, and $\tilde{\mathbf{v}}_{k+N,L}$ is the augmented vector

$\tilde{\mathbf{v}}_{k+N,L} \triangleq \begin{bmatrix} 1 & \mathbf{v}_{k+N,L}^\top \end{bmatrix}^\top$. To account for prediction uncertainties, white Gaussian noise is added to (8) from

$$\boldsymbol{\varepsilon}_k \sim \mathcal{N}(0, \sigma_\varepsilon^2), \quad (9)$$

where σ_ε^2 is considered constant. The noise variance can be estimated through Monte Carlo simulations using the consequent parameters' covariance matrix estimated via RLS until time instant k [3]. We provide a way to recursively track the covariance of estimation errors through the online learning operation, i.e., for time instances $n \in \mathbb{N}_{\leq k}$. The mean error is recursively tracked as

$$\Delta_{\boldsymbol{\varepsilon},n} = \boldsymbol{\varepsilon}_n - \hat{\boldsymbol{\mu}}_{\boldsymbol{\varepsilon},n-1}, \quad (10)$$

$$\hat{\boldsymbol{\mu}}_{\boldsymbol{\varepsilon},n} = \hat{\boldsymbol{\mu}}_{\boldsymbol{\varepsilon},n-1} + \frac{1}{n} \Delta_{\boldsymbol{\varepsilon},n}, \quad (11)$$

in which n is the total number of instances processed by the EFS. The initial mean error is $\hat{\boldsymbol{\mu}}_{\boldsymbol{\varepsilon},0} = \mathbf{0}_{n_y \times 1}$ – where $n_y = 1$ in this case. Given the estimated mean error, the sum of squares is obtained recursively from

$$\mathbf{M}_{\boldsymbol{\varepsilon},n} = \mathbf{M}_{\boldsymbol{\varepsilon},n-1} + (\boldsymbol{\varepsilon}_n - \hat{\boldsymbol{\mu}}_{\boldsymbol{\varepsilon},n-1})(\boldsymbol{\varepsilon}_n - \hat{\boldsymbol{\mu}}_{\boldsymbol{\varepsilon},n-1})^\top, \quad (12)$$

being $\mathbf{M}_{\boldsymbol{\varepsilon},0} = \mathbf{0}_{n_y \times n_y}$. The error covariance matrix at time instant n is

$$\boldsymbol{\Sigma}_{\boldsymbol{\varepsilon},n} = \frac{\mathbf{M}_{\boldsymbol{\varepsilon},n}}{n-1}. \quad (13)$$

The variance σ_ε^2 in (9), used for long-term prediction, is then approximated by

$$\sigma_\varepsilon^2 \approx \boldsymbol{\Sigma}_{\boldsymbol{\varepsilon},k}. \quad (14)$$

3.2 Uncertainty propagation

After obtaining the initial uncertainty in one step estimates (Section 3.1), its long term propagation considers the input vector (3) to be a vector composed of estimated random variables. Note that if $N = 1$, the previous degradation states are known and, naturally, are non-random variables. Accordingly, the output $\hat{\mathbf{x}}_{k+N}$ of the state transition relation (8) is also a random variable,

$$\hat{\mathbf{x}}_{k+N}^+ = \mathbf{h}_k^\top(\mathbf{z}_{k+N}) \hat{\Theta}_k^\top \tilde{\mathbf{v}}_{k+N,L}^+ + \boldsymbol{\varepsilon}_{k+N}, \quad \forall N > 0 \quad (15)$$

where $\mathbf{z}_{k+N} \triangleq \mathbb{E}[\tilde{\mathbf{v}}_{k+N,L}^+]$ are premise variables defined as the expected input vector. Computing variances in a multi-step prediction framework is needed for uncertainty propagation. The first step gives

$$\text{Var}(\hat{\mathbf{x}}_{k+1}^+) = \text{Cov}\left(\mathbf{h}_k^\top(\mathbf{z}_{k+1}) \hat{\Theta}_k^\top \tilde{\mathbf{v}}_{k+1,L}^+\right) + \sigma_\varepsilon^2. \quad (16)$$

As rule activation degrees, $\mathbf{h}_k(\cdot)$, are computed based on the expected value of the random variable $\tilde{\mathbf{v}}_{k+1,L}^+$,

then they can be considered constant; similar to the parameters vector. Let

$$\Xi_N \triangleq \mathbf{h}_k^\top (\mathbf{z}_{k+N}) \hat{\Theta}_k^\top. \quad (17)$$

Thus it is easy to notice that Eq. (16) is rewritten as:

$$\begin{aligned} \text{Var}(\hat{x}_{k+1}^+) &= \Xi_1 \text{Cov}(\tilde{\mathbf{v}}_{k+1,L}^+) \Xi_1^\top + \sigma_\varepsilon^2 \\ &= \Xi_1 \Lambda_1^L \Xi_1^\top + \sigma_\varepsilon^2 \\ &= \sigma_\varepsilon^2 \\ &= \lambda_1^2, \end{aligned} \quad (18)$$

in which $\Lambda_N^L \triangleq \text{Cov}(\tilde{\mathbf{v}}_{k+N,L}^+)$, and $\lambda_N^2 \triangleq \text{Var}(\hat{x}_{k+N}^+)$. Note that $\Lambda_1^L = 0$, since previous degradation states are known at $N = 1$. Then the ***N*-step variance** is computed recursively as

$$\text{Var}(\hat{x}_{k+N}^+) = \Xi_N \Lambda_N^L \Xi_N^\top + \sigma_\varepsilon^2. \quad (19)$$

The covariance matrix of the random vector $\tilde{\mathbf{v}}_{k+1,L}^+$ is

$$\Lambda_N^L = \begin{bmatrix} 0 & 0 & \cdots & 0 \\ 0 & \lambda_{N-1}^2 & \cdots & \lambda_{N-L} \lambda_{N-1} \hat{\rho}_{L,1} \\ \vdots & \vdots & \ddots & \vdots \\ 0 & \lambda_{N-1} \lambda_{N-L} \hat{\rho}_{1,L} & \cdots & \lambda_{N-L}^2 \end{bmatrix}, \quad (20)$$

where the first row and column contain zeros by default, due to matrix augmentation. Moreover, $\lambda_i^2 = 0$ when $i < 0$, meaning that x_{k+N} is known. The covariance matrix (20) is weighted by Pearson correlation coefficients, $\hat{\rho}$, estimated by means of available UUT data.

Considering the degradation to be a random variable with Gaussian distribution, whose expected value is propagated by successive iterations of (8), then RUL lower and upper bounds at an $(\alpha)(100)\%$ significance level are given as

$$\hat{r}_{\text{lower},k} = \inf \{N \in \mathbb{N} : \hat{x}_{k+N} + z_{1-\alpha/2} v_N \geq \eta\}, \quad (21a)$$

$$\hat{r}_{\text{upper},k} = \inf \{N \in \mathbb{N} : \hat{x}_{k+N} + z_{\alpha/2} v_N \geq \eta\}. \quad (21b)$$

Representing, quantifying, forward propagating, and managing uncertainty are issues of utmost importance to support decision-making in practical engineering applications [26]. Nevertheless, there is a lack of effective uncertainty quantification approaches for multi-step prediction based on EFS, where the number of rules starts from scratch and vary over time. In this sense, the uncertainty quantification method described in this section, despite its relative simplicity, is an original contribution to evolving fuzzy modeling. The method enables fault prognostics in dynamic and time-varying environment.

4 Experimental setup

The case study reported in this section concerns the degradation of Li-ion batteries. This type of battery is found in industry and commercially, e.g., in electric vehicles, microgrids, and electronic devices [21, 25]. The cycle aging datasets of four Li-ion batteries are provided by a testbed in the NASA Ames Prognostics Center of Excellence (PCoE). The testbed comprises commercial Li-ion 18650-sized rechargeable batteries from the Idaho National Laboratory; a programmable 4-channel DC electronic load and power supply; voltmeters, ammeters, and a thermocouple sensor suite; custom electrochemical impedance spectrometry equipment; and environmental chamber to impose different operational conditions. The batteries run at room temperature (23° C). Charging is done in constant mode at 1.5 A, until the voltage reaches 4.2 V. Discharging is performed at a constant current level of 2 A, until the battery voltage reaches 2.7 V [25].

The health index (HI) used in the experiments is the percentage charge capacity. When the batteries reach a 30% deterioration in rated capacity (from 1.4 to 2 Ah), experiments are terminated [25]. Therefore, the FT is 70%. Figure 2 summarizes the datasets, namely, B0005, B0006, B0007, and B0018. The dataset B0006 is arbitrarily chosen as the training dataset. We compare three EFSs with each other and with a non-evolving method based on an Autoregressive Moving Average (ARMA) model.

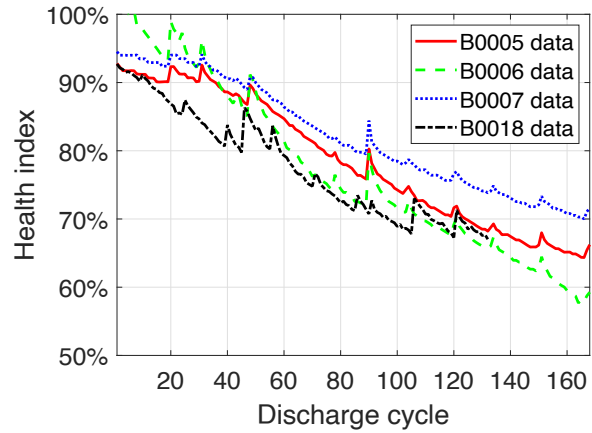


Figure 2: Percentage charge capacity along discharge cycles.

4.1 Parameter tuning

Default hyperparameters were chosen for the different algorithms to be compared. For the EBeTS approach, the choice is based on problem-agnostic recommendations [3]. The EBeTS hyperparameters are

$\omega_{\text{EBETS}} = 95.45\%$, $\tau_{\text{EBETS}} = \ell + 1$, $\gamma_{\text{EBETS}} = 0.5$, and $\delta_{\text{EBETS}} = 10^3$, with ℓ being the number of input lags or autoregressors. The exTS approach depends on the rule covariance initialization constant, Ω_{exTS} , whose meaning is analogous to that of δ_{EBETS} ; therefore $\Omega_{\text{exTS}} = 10^3$. The eMG approach uses as learning rate $\beta_{\text{eMG}} = 0.05$; the unilateral confidence interval to define the eMG compatibility threshold is $\alpha_{\text{eMG}} = 0.01$, the window size for the alert mechanism is $w_{\text{eMG}} = 20$, and the initial dispersion matrix to create clusters is $\Sigma_{\text{eMG}}^{\text{init}} = 10^{-3} \times \mathbf{I}_\ell$.

The number of input lags ℓ is a free parameter to be optimized based on accuracy indices, namely, Relative Accuracy (RA) and Mean Absolute Percentage Error (MAPE). They are computed as follows [27]:

$$\text{MAPE}_k = \frac{100}{N} \sum_{i=k+1}^{k+N} \left| \frac{x_i - \hat{x}_i}{x_i} \right|, \quad (22)$$

$$\text{RA}_k = 1 - \frac{|r_k - \hat{r}_k|}{r_k}, \quad (23)$$

where N is the number of forthcoming predictions until the UUT state reaches the threshold; r_k and \hat{r}_k are the actual and estimated RUL at k , respectively.

The training data, i.e., the data from B0006, and 20 samples of each test dataset, are used to validate a proper number of lags for each modeling approach. Let $I_k(\cdot)$ be

$$I_k(\ell, \zeta, \varkappa) = \text{RA}_k(\ell, \zeta, \varkappa) + \left(1 - \frac{\text{MAPE}_k(\ell, \zeta, \varkappa)}{100} \right) + \left(1 - \frac{\ell}{20} \right), \quad (24)$$

where $\zeta \in \{\text{B0006}, \text{B0007}, \text{B0018}\}$ is a testing battery; $\varkappa \in \{\text{EBETS}, \text{exTS}, \text{ARMA}, \text{eMG}\}$ is an algorithm; and $\ell \in [1, 20]$ is the number of lags. ARMA models consider p and q within $[1, 10]$. The number of lags arises as a result of the following maximization problem,

$$\ell(\zeta, \varkappa) = \arg \max_l \frac{1}{4} \sum_{j \in \{5, 10, 15, 20\}} I_j(\ell, \zeta, \varkappa). \quad (25)$$

Index $I_k(\cdot)$ (24) depends on the actual RUL of a testing battery to compute RA_k . We propose an approximation for validation purpose based on a relation commonly used to quantify the charge capacity of Li-ion batteries,

$$C(k; \mathbf{c}) = c_1 \exp c_2 k + c_3 \exp c_4 k, \quad (26)$$

in which the parameters' vector, $\mathbf{c} = [c_1 \ c_2 \ c_3 \ c_4]^\top$, is given using the known data from a battery and the least-squares method.

The function `lsqcurvefit`¹ is used to find the parameters' vector \mathbf{c} in (26) for the training battery B0006, which are used as a starting point to estimate the parameters of the same exponential model (26) for the test batteries. RUL estimates for each test battery take the average between the model developed from the training data B0006 and the model found based on the first 20 test samples. Overall and average results are exemplified in Figure 3. The same procedure is applied to batteries B0007 and B0018.

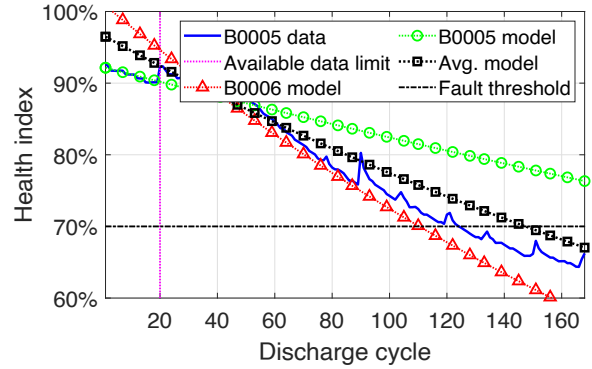


Figure 3: Combined exponential model using B0006 model and B0005 partial model.

The parameters of the exponential relation (26), as portrayed by the data in Figure 3, are listed in Table 1. To find the parameters in Table 1 using B0006 training data, the least-squares starting point is $\mathbf{c}_0 = [1 \ 1 \ 1 \ 0]^\top$. For the other batteries, the final coefficients for the B0006 model are used as starting point.

Table 1: Least-squares fit of the exponential models' parameters based on battery charge capacity data.

Battery	c_1	c_2	c_3	c_4
B0006	-0.4512	13.3905	1.0115	0.0033
B0005	-0.4512	13.3905	0.9226	0.0011
B0007	-0.4512	13.3905	0.9437	0.0010
B0018	-0.4512	13.3905	0.9305	0.0031

After defining the parameters of (26) for each test dataset, RUL estimates are given and the index I_k (24) is computed. With $I_j \forall j$ in hands, we maximize (25) to obtain the optimal number of lags. In particular, given the data ζ related to a battery, and an algorithm \varkappa , the following steps are performed to find the optimal number of lags:

1. Find the parameters of an instance of (26) using the training data, B0006;

¹Available in <https://www.mathworks.com/help/optim/ug/lsqcurvefit.html>

2. Find the parameters of an instance of (26) using the test data of battery ζ , i.e., the first 20 samples of the respective dataset;
3. Provide a RUL estimate using the average of the predictions given by the models from Steps 1 and 2;
4. For the different amounts of lags, from 2 to 20, manipulate the training data, B0006, using a Hankel matrix, accordingly;
5. Use algorithm \varkappa to train a model for each amount of lags based on the data from Step 4;
6. Solve the maximization problem (25) to find the optimal number of lags, and optimal model.

5 Results and discussion

The optimization problem (25) defines the number of input lags for each algorithm-battery pair. The third column of Table 2 shows the number of lags chosen for each pair; the subsequent columns show the RA for different starting prognostics points t_P . The symbol ‘*’ indicates that the prognostics task was not carried out for the t_P . Additionally, ‘-’ means the infeasibility of an algorithm to compute the RUL for the t_P . Infeasibility happens if long-term predictions converge to a value greater than the FT, or have their slope changed to positive, thus never reaching the FT. Notice that the lag column in Table 2 for ARMA models corresponds to the parameter p , whereas the q coefficient is zero for all cases, as found in validation. To compare algorithms fairly, the sample index (s_i) in which the prognostics start is set considering the t_P and the number of input lags of each battery-algorithm pair. Using the EBeTS algorithm as a basis, then $s_i = t_P - (\ell - 3)$. For this reason, the B0018-exTS pair is unable to start the prognostics task at $t_P = 20$, since $s_i = 6$ is less than $\ell = 17$.

Table 2 indicates that multivariate Gaussian models can better capture the information in some datasets. For instance, EBeTS and eMG have shown similar results for battery B0005. However, this is not observed for batteries B0007 and B0018, in which non-evolving ARMA models may eventually perform better. In general, different initial hyperparameters for the different algorithms may lead to slightly different results. In the absence of a fine-tuning procedure to set initial hyperparameters, evolving algorithms are more prone to develop sub-optimal models in the sense of long-term trends. Nevertheless, we highlight that EBeTS hyperparameters come from a problem-agnostic methodology, i.e., from a method that does not require expert knowledge about the problem.

Table 2: RA for algorithm-battery pairs with prognostics starting at different t_P . Best values are in bold.

Bat.	Alg.	ℓ	t_P				
			20	40	60	80	100
B0005	EBeTS	3	0.94	0.78	0.76	0.98	0.96
	fails at	exTS	9	-	-	-	0.95 0.91
	cycle	ARMA	1	0.77	0.83	0.86	0.74 0.82
	125	eMG	5	0.89	0.98	0.94	0.91 0.96
B0007	EBeTS	3	0.82	0.89	0.84	0.72	0.75
	fails at	exTS	10	0.69	0.55	-	- 0.83
	cycle	ARMA	1	0.59	0.62	0.57	0.51 0.52
	166	eMG	5	0.69	0.76	0.71	0.63 -
B0018	EBeTS	3	0.91	0.96	0.79	0.79	*
	fails at	exTS	17	*	0.59	-	- *
	cycle	ARMA	1	0.80	0.78	0.91	0.57 *
	97	eMG	5	0.84	0.89	-	- *

* prognostics task not performed.

- algorithm’s infeasibility to give the RULs.

The $\alpha - \lambda$ plot for battery B0005 is shown in Figure 4. The uncertainty is quantified for all evolving models using the online error tracking method with a 99% confidence level. Uncertainty propagation within ARMA models² yields too wide confidence intervals. Their bounds enclose the whole goal region, which is quite little useful to assist decision making. Similarities between EBeTS and eMG, as noticed in Table 2, is also perceived from Figure 4 for battery B0005. These methods provided the narrowest confidence intervals. In some experiments, the estimated RUL (red line) is missing. In these cases, the long-term prediction does not reach the FT, as discussed previously.

Figure 5 shows the long-term prediction for battery B0005 and $t_P = 20$, see dashed black line. The dashed red line is the expected HI propagated multiple steps ahead, while the dash-dotted black lines are its confidence intervals. In the ARMA and exTS cases, such uncertainty interval becomes large enough to provide poor decision-making support, which is not the case for the remaining methods since they consider relationships among input features.

6 Conclusion

EFSs are promising methods to deal with nonlinear problems in non-stationary environments. Their structures are flexible, and their parameters can be updated recursively according to data stream changes. Structural learning from scratch, rapid recursive updates, and historical-data storage avoidance make EFSs quite suitable to be used in real-time prognostics systems. We have shown the effectiveness of EFSs, namely

²A built-in function of the MATLAB System Identification Toolbox. Available in <https://www.mathworks.com/help/ident/ref/forecast.html>

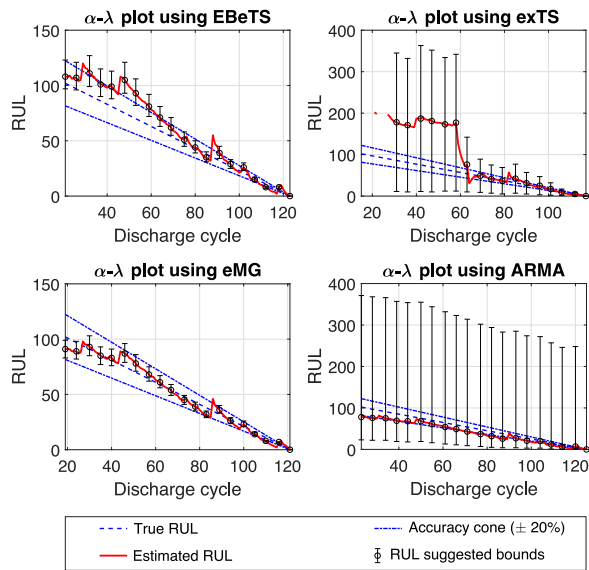


Figure 4: $\alpha - \lambda$ plot of the estimated RUL of battery B0005. The goal region is $\alpha = 0.2$.

EBETS and eMG, in comparison to exTS and ARMA models, using a real-world benchmark dataset concerning the prognostics of charge capacity of Li-ion batteries. EFSs-based models have offered online condition monitoring and a way of fusing multivariate data streams aiming at describing the multiple-stage battery-degradation phenomenon and providing prognostics. Furthermore, a framework to quantify and propagate uncertainties related to estimation errors has been improved to produce smooth confidence intervals. The proposed uncertainty quantification framework can be plugged into any EFS for real-time prognostics.

Acknowledgement

This work was supported in part by the Brazilian agencies CNPq, FAPEMIG, CAPES, and in part by the PROPG-CAPES/FAPEAM Scholarship Program.

References

[1] D. An, N. H. Kim, J. H. Choi, Practical options for selecting data-driven or physics-based prognostics algorithms with reviews, *Reliab. Eng. Syst. Saf.* 133 (2015) 223–236.

[2] P. Angelov, X. Zhou, Evolving fuzzy systems from data streams in real-time, in: *Int. Symposium on Evolving Fuzzy Systems*, IEEE, 2006.

[3] M. O. Camargos, I. Bessa, M. F. S. V. D’Angelo, L. B. Cosme, R. M. Palhares, Data-driven prognostics of rolling element bearings using a novel

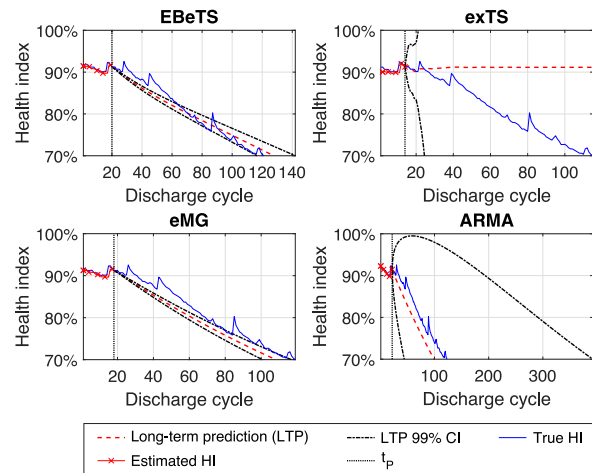


Figure 5: Long-term prediction, with 99% confidence, of the different methods for Battery B0005.

error based evolving takagi–sugeno fuzzy model, *Applied Soft Computing* 96 (2020) 106628.

[4] J. Chiachío, M. Chiachío, S. Sankararaman, A. Saxena, K. Goebel, Condition-based prediction of time-dependent reliability in composites, *Reliab. Eng. Syst. Saf.* 142 (2015) 134–147.

[5] S. L. Chiu, Fuzzy model identification based on cluster estimation, *Journal of Intelligent and Fuzzy Systems* 2 (3) (1994) 267–278.

[6] L. A. Q. Cordovil, P. H. S. Coutinho, I. V. Bessa, M. F. S. V. D’Angelo, R. M. Palhares, Uncertain data modeling based on evolving ellipsoidal fuzzy information granules, *IEEE Transactions on Fuzzy Systems* 28 (10) (2020) 2427–2436.

[7] L. B. Cosme, W. M. Caminhas, M. F. S. V. D’Angelo, R. M. Palhares, A Novel Fault-Prognostic Approach Based on Interacting Multiple Model Filters and Fuzzy Systems, *IEEE Trans. Ind. Electron.* 66 (1) (2019) 519–528.

[8] A. Cubillo, S. Perinpanayagam, M. Esperon-Miguez, A review of physics-based models in prognostics: Application to gears and bearings of rotating machinery, *Advances in Mechanical Engineering* 8 (8) (2016) 1–21.

[9] M. El-Koujok, R. Gouriveau, N. Zerhouni, Reducing arbitrary choices in model building for prognostics: An approach by applying parsimony principle on an evolving neuro-fuzzy system, *Microelectronics Reliability* 51 (2) (2011) 310–320.

[10] R. Gouriveau, N. Zerhouni, Connexionist-systems-based long term prediction approaches

- for prognostics, *IEEE Transactions on Reliability* 61 (4) (2012) 909–920.
- [11] A. K. S. Jardine, D. Lin, D. Banjevic, A review on machinery diagnostics and prognostics implementing condition-based maintenance, *Mech. Syst. Signal Process.* 20 (7) (2006) 1483–1510.
- [12] M. Jouin, R. Gouriveau, D. Hissel, M. C. Péra, N. Zerhouni, Particle filter-based prognostics: Review, discussion and perspectives, *Mech. Syst. Signal Process.* 72-73 (2016) 2–31.
- [13] M. S. Kan, A. C. C. Tan, J. Mathew, A review on prognostic techniques for non-stationary and non-linear rotating systems, *Mechanical Systems and Signal Processing* 62 (2015) 1–20.
- [14] N. K. Kasabov, Q. Song, DENFIS: dynamic evolving neural-fuzzy inference system and its application for time-series prediction, *IEEE T FUZZY SYST* 10 (2) (2002) 144–154.
- [15] Y. Lei, N. Li, L. Guo, N. Li, T. Yan, J. Lin, Machinery health prognostics: A systematic review from data acquisition to RUL prediction, *Mechanical Systems and Signal Processing* 104 (May) (2018) 799–834.
- [16] D. Leite, R. M. Palhares, V. C. S. Campos, F. Gomide, Evolving granular fuzzy model-based control of nonlinear dynamic systems, *IEEE Transactions on Fuzzy Systems* 23 (4) (2015) 923–938.
- [17] D. F. Leite, M. B. Hell, P. Costa, F. Gomide, Real-time fault diagnosis of nonlinear systems, *Nonlinear Analysis: Theory, Methods & Applications* 71 (12) (2009) e2665–e2673.
- [18] A. Lemos, W. Caminhas, F. Gomide, Multivariable gaussian evolving fuzzy modeling system, *IEEE T FUZZY SYST* 19 (1) (2011) 91–104.
- [19] A. Lemos, W. Caminhas, F. Gomide, Adaptive fault detection and diagnosis using an evolving fuzzy classifier, *Inf. Sci.* 220 (2013) 64–85.
- [20] N. Li, Y. Lei, J. Lin, S. X. Ding, An Improved Exponential Model for Predicting Remaining Useful Life of Rolling Element Bearings, *IEEE Trans. Ind. Electron.* 62 (12) (2015) 7762–7773.
- [21] X. Li, Z. Wang, J. Yan, Prognostic health condition for lithium battery using the partial incremental capacity and Gaussian process regression, *J. Power Sources* 421 (February) (2019) 56–67.
- [22] A. T. Nguyen, T. Taniguchi, L. Eciolaza, V. Campos, R. Palhares, M. Sugeno, Fuzzy control systems: Past, present and future, *IEEE Comput. Intell. Mag* 14 (1) (2019) 56–68.
- [23] Y. Peng, M. Dong, M. J. Zuo, Current status of machine prognostics in condition-based maintenance: A review, *Int. J. Adv. Manuf. Technol.* 50 (1-4) (2010) 297–313.
- [24] E. Ramasso, T. Denoeux, Making use of partial knowledge about hidden states in HMMs: An approach based on belief functions, *IEEE Transactions on Fuzzy Systems* 22 (2) (2014) 395–405.
- [25] B. Saha, K. Goebel, Modeling li-ion battery capacity depletion in a particle filtering framework, in: *Proceedings of the annual conference of the prognostics and health management society, 2009*, pp. 2909–2924.
- [26] S. Sankararaman, Significance, interpretation, and quantification of uncertainty in prognostics and remaining useful life prediction, *Mechanical Systems and Signal Processing* 52-53 (1) (2015) 228–247.
- [27] A. Saxena, J. Celaya, E. Balaban, K. Goebel, B. Saha, S. Saha, M. Schwabacher, Metrics for evaluating performance of prognostic techniques, *2008 International Conference on Prognostics and Health Management, PHM 2008*.
- [28] X. S. Si, W. Wang, C. H. Hu, M. Y. Chen, D. H. Zhou, A Wiener-process-based degradation model with a recursive filter algorithm for remaining useful life estimation, *Mechanical Systems and Signal Processing* 35 (1-2) (2013) 219–237.
- [29] D. A. Tobon-Mejia, K. Medjaher, N. Zerhouni, G. Tripot, A Data-Driven Failure Prognostics Method Based on Mixture of Gaussians Hidden Markov Models, *IEEE Transactions on Reliability* 61 (2) (2012) 491–503.
- [30] R. R. Yager, A model of participatory learning, *IEEE Transactions on Systems, Man, and Cybernetics* 20 (5) (1990) 1229–1234.